

Effect of TiO₂-ZnO/GAC on by-product distribution of CVOCs decomposition in a NTP-assisted catalysis system

Kamaladdin Abedi^{1,2}, Farshid Ghorbani-Shahna^{2,*}, Abdolrahman Bahrami², Babak Jaleh³, Rasoul Yarahmadi⁴

¹Kurdistan University of Medical Sciences, Department of Occupational Health Engineering, Faculty of Health, Sanandaj, Iran

²Hamedan University of Medical Sciences, Center of Excellence for Occupational Health, Research Center for Health Sciences, Hamedan, Iran

³Bu-Ali Sina University, Department of physics, Hamedan, Iran

⁴Iran University of Medical Sciences, Department of occupational health, Occupational health research center, School of public health, Tehran, Iran

*Corresponding author: e-mail: fghorbani@umsha.ac.ir

In this study, the catalytic effect of TiO₂-ZnO/GAC coupled with non-thermal plasma was investigated on the by-products distribution of decomposition of chlorinated VOCs in gas streams. The effect of specific input energy, and initial gas composition was examined in a corona discharge reactor energized by a high frequency pulsed power supply. Detected by-products for catalytic NTP at 750 J L⁻¹ included CO, CO₂, Cl₂, trichloroacetaldehyde, as well as trichlorobenzaldehyde with chloroform feeding, while they were dominated by CO, CO₂, and lower abundance of trichlorobenzaldehyde and Cl₂ with chlorobenzene introduction. Some of the by-products such as O₃, NO, NO₂, and COCl₂ disappeared totally over TiO₂-ZnO/GAC. Furthermore, the amount of heavy products such as trichlorobenzaldehyde decreased significantly in favor of small molecules such as CO, CO₂, and Cl₂ with the hybrid process. The selectivity towards CO_x soared up to 77% over the catalyst at 750 J L⁻¹ and 100 ppm of chlorobenzene.

Keywords: non-thermal plasma, catalyst, CVOCs, TiO₂-ZnO, granular activated carbon.

INTRODUCTION

Chlorinated volatile organic compounds (CVOCs) are a group of hazardous atmospheric emissions that can harm both human and environment¹. According to the International Agency for Research of Cancer, some of these compounds have been classified in the group of possibly carcinogenic to human². They are also a major threat to global warming³. Several legislations and limit values have been recently established in many countries including developing countries^{4,5} in order to restrict the release of these hazardous compounds into atmosphere, and using more efficient technologies has therefore become obligatory. Based on the literature, non-thermal plasma (NTP) can effectively decompose CVOCs in a gas medium^{6,7}. However, due to the formation of many harmful by-products employing this technique alone lies into several limitations. Instead, a NTP-catalysis hybrid process has been recently suggested, believing that it leads to both higher removal efficiency, and much better by-products distribution^{8,9}. Nevertheless, searching to find a suitable catalyst which shows the best catalytic activity and also by-products selectivity in combination with NTP is still going on¹⁰. When CVOCs are decomposed, the ideal products are CO₂, H₂O, HCl, as well as Cl₂. But, incomplete destruction of CVOCs may lead to some undesirable by-products which can be more toxic than the original compounds^{1,11}. The mechanisms of CVOCs degradation and the identification of by-products are of paramount importance, since this information can be used in better designing of the NTP processes and particularly choosing appropriate catalyst. In recent years, the mechanism of VOCs decomposition has attracted some interest^{12,13}, although little and rare attention has been paid to NTP-assisted technique and CVOCs.

Based on the literature, if metal oxide nanoparticles are used in mixtures, their catalytic activity will be improved considerably¹⁴. Impregnation of semiconductor catalysts on adsorbents can also lead to increase the catalytic performance significantly¹⁰. The higher reaction rates resulting from the above-mentioned points can be in favor of less harmful by-products due to the destruction of initial hazardous intermediates generated inside the plasma reactor^{15,16}. In the present study, therefore, TiO₂ and ZnO nanoparticles were coated on GAC as a substrate to obtain such results. In addition, the effect of these catalysts coupled with plasma process was investigated on the chloroform and chlorobenzene conversion which has rarely been reported in scientific literature^{16,17}. Special attention was given to the mechanism of CVOCs decomposition and their by-products distribution using GC/MS and direct reading instruments data.

EXPERIMENTAL

Experimental apparatus

A schematic diagram of the experimental set-up is shown in Figure 1. It is seen from the figure that normal air was passed through an air filter using an air compressor to be cleaned and dried. This air was then flowed through a chamber and mixed with the injected liquids. Afterwards, the polluted gas was fed into the reactors. The background gas temperature was kept at 40°C employing a temperature controller to vaporize the volatile liquids effectively. JMS SP-510 (Japan) syringe pumps were used for liquids to be injected into the gas stream, and a favorable concentration of the pollutants (100–700 ppm) was provided. The gas flow rate was controlled using two needle valves and kept constant

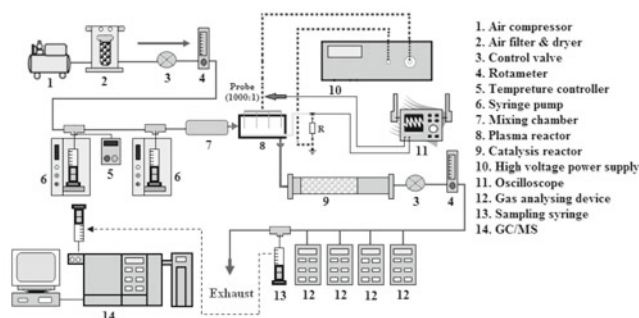


Figure 1. Schematic diagram of the experimental set-up in the range of 0.2–1 L min⁻¹. Finally, a small chamber and some direct reading instruments were placed in-line for the gas to be analyzed.

Reagents

All the chemicals used (analytical grade), were purchased from Merck (Germany) except for tetra-*n*-butyl titanate which was supplied from Fluka (Switzerland).

Catalyst preparation

The catalysts were prepared using dip-coating technique which was performed by a sol-gel process at low temperature of 75°C. The detailed procedure for TiO₂ sol preparation is given in Ref.¹⁸. The ZnO sol was also prepared as follows: after dissolving 8.76 g of zinc acetate dehydrate in 200 ml of ethanol, the resultant was stirred in a water bath at 50°C, followed by adding 5.96 g of tri-ethanol amine and continued to stir for 1 h. Afterwards, the mixture was placed under vibration and heat treatment for 0.5 h at 40°C. For ZnO/GAC to be obtained, 6 g of GAC was added to the resultant ZnO sol, and then vibrated, filtered, dried, and followed by calcination for 4 h at 300°C. 3 g of this ZnO/GAC was then added to 100 ml of TiO₂ sol, and allowed to vibrate for 0.5 h. After filtration, drying, and calcination for 2 h at 400°C, TiO₂-ZnO/GAC was resulted.

Plasma and catalyst reactors

A pin-to-plate corona discharge reactor made up of quartz formed as a rectangular tube with 20×15×200 mm dimensions was used as plasma source. The reactor also consisted of 6 stainless steel needles as discharge electrodes and an aluminum foil as a single ground electrode. The electrodes were placed at a distance of 7 mm from each other. The applied electric current was divided equally between 6 discharge needles using a resistance box. The reactor was designed to form small tunnels near pin electrodes, so that the air was allowed to pass as close as possible to the discharge zone, and as a result the reactor volume became smaller and calculated to be 20 ml. A cylindrical quartz tube with 15×100 mm dimensions, locating immediately after the NTP reactor, was also employed as catalyst reactor. Catalyst particles were prevented to escape using two stainless steel meshes with some amounts of glass wool positioned at both ends of the tube. 3 g of catalyst was used for each experiment.

Power supply system and electrical measurements

A high voltage and frequency pulsed transformer (Effective voltage = 6–16 kV, effective current = 0–15 mA,

effective frequency = 1–18 kHz) was connected to the discharge electrodes to generate NTP. Negative and positive pulses were applied to the discharge electrodes with a rising and duration time of 200 ns and 2 μs respectively. Typical voltage and current waveforms is shown in Figure 2. The voltage and current delivered into the Plasma reactor were measured using an oscilloscope (HAMEG HM 203-7 Germany). A high voltage probe (1000:1) was employed for voltage measurements. The current was also measured applying a resistor ($R = 50\Omega$) and a cable which was connected to the oscilloscope. Specific input energy (SIE) as an indicator of the energy delivered to the reactor was calculated as expressed in Eq. 1. Integrating the voltage and current products in one pulse duration gives the energy consumed in a pulse time, which can then be multiplied by the pulse frequency to obtain the discharge power in a second. Afterwards, this discharge power was divided by the gas flow rate, yielding SIE.

$$SIE(J/L) = \frac{\left[\int |V(t) \times I(t) dt| \right] (J/Pulse) \times Pulse\ frequency (Pulse/S)}{Gas\ flow\ rate (L/S)} \quad (1)$$

Due to the beneficial effect of pulse repetition frequency which was determined in our pretests, SIE was varied by only changing the voltage amplitude and frequency was set at its maximum value during all experiments.

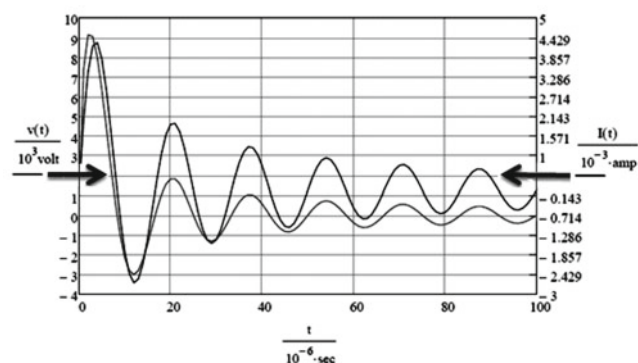


Figure 2. Typical voltage and current waveforms at applied voltage of 9 kV

Gas analysis

The influent and effluent gas were analyzed before and after the catalytic plasma process by using a Varian 3800 GC equipped with a Saturn 2200 mass spectroscopy system (GC/MS). The GC was also equipped with a SGE capillary column with the inner diameter of 0.22 mm, film diameter of 0.25 μm, and length of 25 m. For each experiment, one ml of gas was sampled. NO and NO₂ were monitored employing a NO_x meter (G750 polytor, Germany). CO and CO₂ were also detected applying CO (SGA91, U.K.) and CO₂ (Testo535, Germany) analyzers. In order to measure low and high concentrations of ozone, a direct reading instrument (EST-1510, USA) and KI titration technique were used respectively. The temperature and humidity of the system were also recorded utilizing a thermohygrometer (Testoterm, GmbH & Co., Germany). Hydrogen chloride was also quantified using HCl gas detector tubes. Our indicator for degradation rate of contaminated compounds was removal efficiency (RE) which was calculated as shown in equation 2.

$$RE(\%) = \left(1 - \frac{[CVOC]_{out}}{[CVOC]_{in}}\right) \times 100 \quad (2)$$

Where, $CVOC_{out}$ and $CVOC_{in}$ indicate the steady state concentration of CVOCs at the outlet and inlet of the hybrid system, respectively. Then, CO_2 selectivity (S_{CO_2}) is given as follows:

$$S_{CO_2(chloroform)}(\%) = \frac{[CO_2]}{[chloroform]_{in} \times RE} \times 100 \quad (3)$$

$$S_{CO_2(chlorobenzene)}(\%) = \frac{[CO_2]}{6([chlorobenzene]_{in} \times RE)} \times 100 \quad (4)$$

RESULTS AND DISCUSSION

Catalyst properties

the catalysts were subjected to XRD analysis over the 2θ range of $10-80^\circ$. Figure 3 shows the X-ray diffractograms of nanocomposites. As Figure 3 shows, besides the anatase and the species ascribed to the support, no rutile and brookite phases were observed, implying the TiO_2 anatase/GAC composite formation. It is also shown in Figure 3 that a fairly high peak was detected at $2\theta = 26.4$ which can be related to the GAC itself. This most intense peak of the template overlapped strongly the anatase TiO_2 refractogram at 2θ of 25.1 . Furthermore, all diffraction peaks of ZnO correspond to the standard diffraction pattern (Fig. 3).

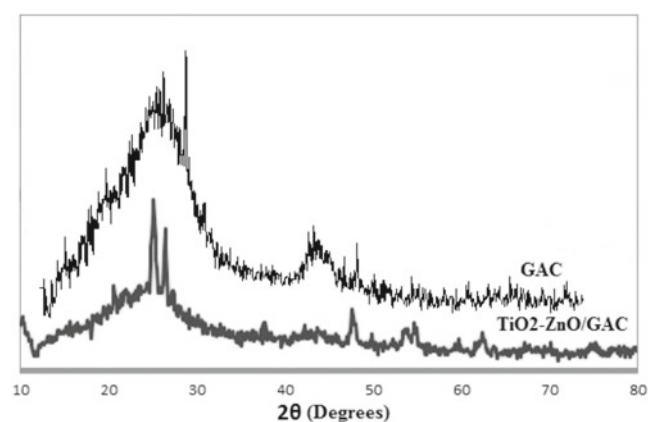
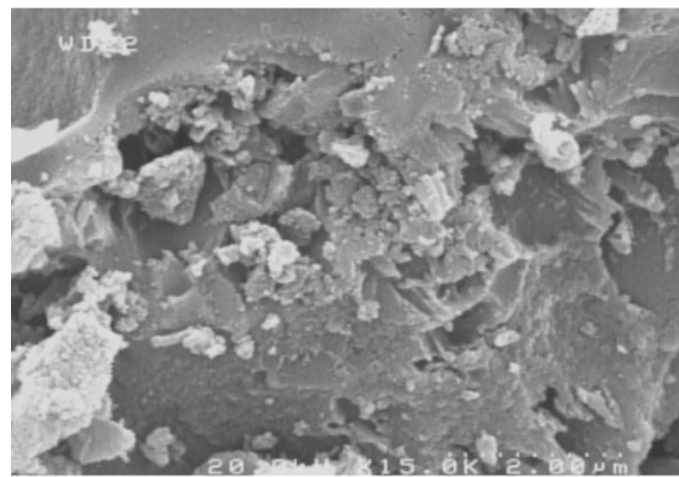
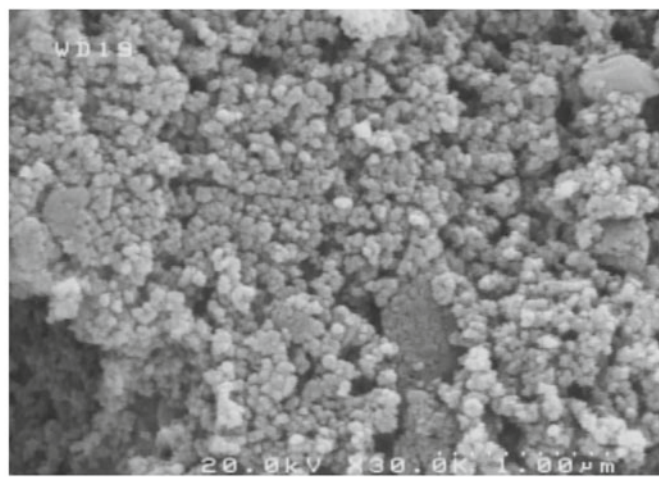


Figure 3. X-ray diffractograms of nanoparticles prepared by sol-gel technique supported on GAC (a) GAC itself, and (b) TiO_2 -ZnO/GAC



(a)



(b)

Figure 4. Top view morphology of catalysts prepared by sol-gel process (a) GAC, and (b) TiO_2 -ZnO/GAC

It is also seen in Figure 3 that the intensity of zinc oxide peaks decreases resulting from the decreased amount of ZnO particles. The larger ZnO particles being coated by the finer TiO_2 nanocrystals may be the reason. SEM observations confirmed the nano size of the prepared particles as Figure 4 represents. The larger size of ZnO particles can be easily noticed in the figure. Agglomeration can be a possible reason¹⁹. A non-uniform structure with a lot of large cavities is obvious for GAC before impregnation (Fig. 4). After impregnation, however, most of the holes were covered by a thin layer of TiO_2 and ZnO formed over the surface, and a smoother and more even surface was obtained. SEM images also show that the quantity of TiO_2 particles is much higher than that of ZnO and the catalyst is affected by TiO_2 much more than ZnO particles. These phenomena may be the consequence of smaller size and crystallinity structure of TiO_2 nanoparticles²⁰.

Removal efficiency results

The voltage amplitude was changed from 6–16 kV and consequently the SIE was varied between 110–1500 $J L^{-1}$. Table 1 presents the experimental results of the NTP alone and catalytic NTP on the CVOCs degradation as a function of SIE. It is evident from Table 1 that increasing SIE contributes to removal efficiency enhancing. Contrary to our expectations, chloroform was oxidized much better than chlorobenzene. The reason is not clearly known, but the difference in the energy needed for the conversion of the two chemicals may due to the difference in the initial dissociative reactions and also the difference in the subsequent chain reactions. The effect of catalyst is obviously significant from Table 1. It can be seen from Table 1 that the introduction of TiO_2 -ZnO/GAC contributes to the dramatic enhancement of the removal efficiency. It also indicates that TiO_2 -ZnO/GAC is extremely activated when an excited gas consisting of a huge amount of ozone is passing through the catalyst bed.

CO and CO_2 selectivity

The production of many organic and non-organic compounds is a known fact in all conversion processes particularly with NTPs. In the present study the distribution and quantity of various by-products was determined through direct measurements. Table 2 represents non-organic products detected during the present study.

Table 1. Chloroform and chlorobenzene removal rate with NTP alone and catalytic NTP as a function of SIE

SIE [J L ⁻¹]	Removal efficiency [%]			
	Chloroform		Chlorobenzene	
	NTP	Catalytic NTP	NTP	Catalytic NTP
110	21.0	74.5	12.9	49.0
240	29.6	79.5	20.2	57.0
300	40.3	85.6	30.0	66.0
400	50.8	90.9	36.7	76.0
550	60.5	98.2	43.2	83.4
750	73.1	99.3	52.7	91.1

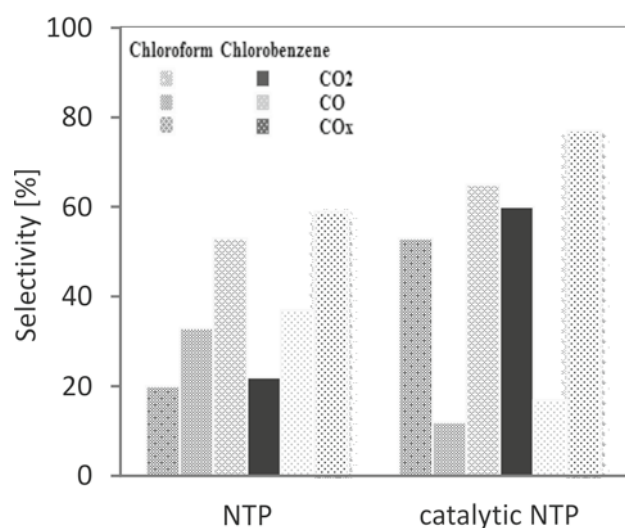
Table 2. Typical non-organic by-products detected during this work

By-product	Chemical formula	Molecular weight	Toxicity
Ozone	O ₃	48	Irritant
Nitrogen oxide	NO	30	Irritant
Nitrogen dioxide	NO ₂	46	Irritant
Carbon monoxide	CO	28	Asphyxiant
Carbon dioxide	CO ₂	44	Asphyxiant
Water	H ₂ O	18	–

These are typical by-products observed with most of NTP studies^{16,21}. The main by-products i.e. CO and CO₂ (CO_x) are shown in Figure 5 at energy density of 750 J L⁻¹ and 100 ppm of pollutants. As Figure 5 represents, applying the NTP-alone process, the CO_x yield was around 60% with chloroform feeding, implying that the products were dominated by CO and CO₂. It means also that about 40% of the removed chloroform appeared as chlorinated and other organic intermediates. When catalyst is present, the concentration of CO₂ and subsequently CO_x increased. From these results, a very high ability of CO removal can be concluded for the catalyst. This effect can be associated with NO_x removal as represented in reaction (1)²², and will be discussed further in the next section.



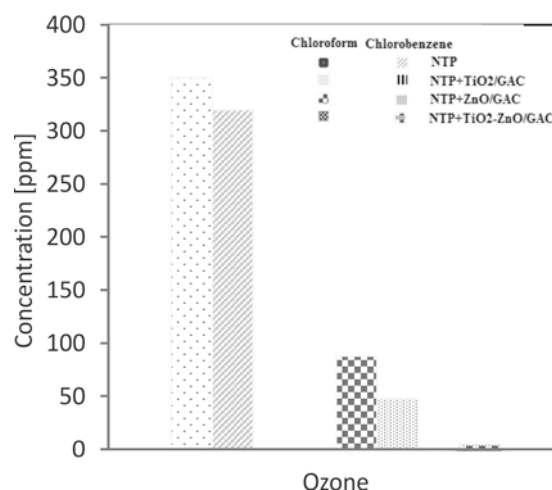
With chlorobenzene, however, some changes occurred and the level of carbon containing products i.e. CO, and CO₂ was higher as compared to the same conditions with chloroform. Figure 5 also shows the CO_x selectivity under the conditions where chlorobenzene fed into the reactor. It is clear from the figure that the CO_x

**Figure 5.** The selectivity towards CO, CO₂, and CO_x with the effect of catalyst (SIE = 750 J L⁻¹, and 100 ppm of CVOCs)

concentration increased over the catalyst, soaring up to 77%. Furthermore, in the presence of catalyst similar observations were made as obtained for chloroform with regard to CO and CO₂ selectivity, where the selectivity towards the former decreased and increased for the latter. These findings may be supported by the study of Marotta et al., in which they declared C₆H₅⁺ and C₄H₃⁺ as the predominant positive ions resulted from the initial fragmentation of chlorobenzene²³. These initial products can be further decomposed into CO, CO₂, as well as H₂O after reaction with active species generated inside NTP reactor and also over catalysts due to ozone dissociation. As will be discussed in the following sections, apart from the residuals of chlorobenzene itself, only two major chlorinated by-products were detected after chlorobenzene conversion in this work, indicating that the chlorobenzene decomposition products were dominated by CO_x. If the concentration of by-products other than CO_x is negligible, the CO_x selectivity could represent carbon balance. As Figure 5 shows, in the presence of TiO₂-ZnO/GAC about 65% of chloroform and 77% of chlorobenzene carbons were oxidized to CO_x. Some of the by-products such as TCBA, TCAA, etc. were quantitatively undetectable using our analysis equipment. Therefore, the exact value of carbon balance cannot be calculated. However, any carbon missing can be attributed to the hydrocarbon retention by the adsorption ability of the catalyst substrate and also to the indistinguishable C containing black soot particles suspended in a water impinger trap positioned downstream of the reactors.

Ozone

Among the other products represented in Table 2, O₃ appears to have a crucial role in two-stage NTP-catalysis processes^{13,24,25}. As Figure 6 shows, the amount of ozone

**Figure 6.** Ozone concentration as a major by-product of NTP process and the effect of catalysts on its destruction (SIE = 750 J L⁻¹, and 100 ppm of CVOCs)

is obviously high with NTP-alone process and reached up to 350 and 320 ppm at 750 J L^{-1} with chloroform and chlorobenzene, respectively. This discrepancy is also seen with increasing the energy density as shown in Figure 7. Partially lower quantity of ozone with chlorobenzene feeding indicates that the gas composition inside the NTP reactor can influence the formation of ozone and some other compounds. A heavier molecule of chlorobenzene is the reason in our view. More energy is consumed to decompose larger molecules and hence the energy density become different, resulting in decreased level of energy delivered to oxygen molecules to produce O_3 . Furthermore, NO_2 quantity was rather lower in the presence of chlorobenzene, indicating that less active N or O species were generated, although with no significant statistical difference with chloroform introduction cases. As Figure 7 shows, ozone was totally removed in the presence of catalyst. The temperature in the gas effluent did not exceed 312 K with both NTP-alone and catalytic NTP, and hence destruction by heat may not be the reason. Furthermore, some amounts of ozone and also NO remained unchanged with TiO_2/GAC , and ZnO/GAC alone. Therefore, the synergy between TiO_2 and ZnO can be considered as an effective factor in causing these positive results. However, unlike the findings of Karupiah et al., when chloroform injected into the reactor, an appreciable ozone destruction activity was also found for TiO_2/GAC in the present study²⁶. Karupiah et al. reported that the ozone molecule cannot be degraded by TiO_2 , and considered other catalysts such as MnOx to have such effect instead. Nevertheless, during this study, a significant decline was observed for ozone concentration after NTP- TiO_2/GAC treatment of chloroform, although without total removal. The observations made with ZnO/GAC integration did not show favorable results in terms of O_3 concentrations. For instance, with chloroform feeding, the level of O_3 was still around 90 ppm. It can be concluded from these points that the removal of both initial and intermediate contaminants can be improved by the higher catalyst ability for O_3 destruction, because,

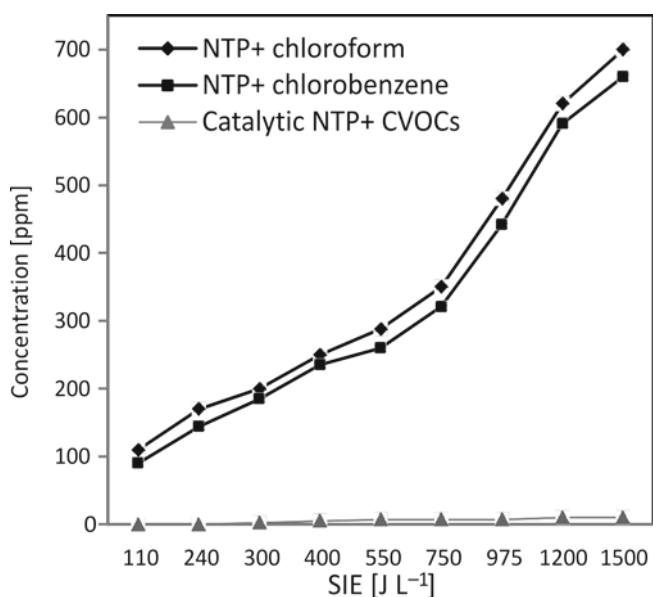
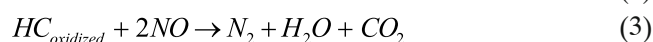
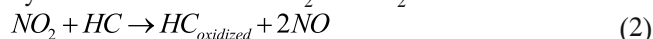


Figure 7. The effect of initial gas feeding on ozone formation with NTP and the hybrid process as a function of SIE

the amount of NO was also considerable downstream of the ZnO/GAC .

NO and NO_2

NO , and NO_2 were also detected as by-products during this study. The concentration of these compounds were considerably high after plasma treatment, and as represented in Figure 8, the amount soared up to ca. 60 and 42 ppm inside the plasma reactor at 750 J L^{-1} for NO and NO_2 respectively. Figure 8 also shows that when the catalysts combined with the NTP, the concentration of NO and NO_2 decreased significantly except with the ZnO/GAC . This implies the ability of catalysts TiO_2/GAC and $\text{TiO}_2\text{-ZnO}/\text{GAC}$ for NO_x abatement. The decomposition of NO_x has been investigated over various catalysts in several previous works²⁷⁻²⁹. From the results of these works, one may conclude that the presence of partially oxidized hydrocarbons can strongly cause NO_x to participate in several redox reactions, leading to the final N_2 formation and also further decomposition of hydrocarbon itself to CO_2 and H_2O ^{28, 29}:



TCBA ($\text{C}_7\text{H}_4\text{Cl}_3\text{O}$) and TCE (C_2HCl_3) may have this role in the present study, since their concentration also decreased noticeably downstream of the catalysts. NO can even undergo a reaction with CO to give N_2 and CO_2 as expressed in reaction (1)²². This could be one of the reaction pathways in this study because CO was also removed significantly after catalysis treatment.

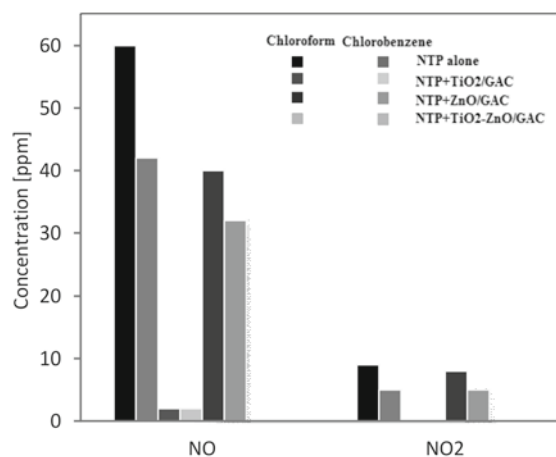


Figure 8. NO_x concentration with NTP and the effect of catalysts on it (SIE = 750 J L^{-1} , and 100 ppm of CVOCs)

Figures 9 and 10 show the NO and NO_2 concentrations generated in the plasma reactor as a function of input energy. It is clear from the Figures that both of these products disappeared over $\text{TiO}_2\text{-ZnO}/\text{GAC}$ regardless of the SIE used. Figure 10 also shows that at input powers less than 450 J L^{-1} , no NO_2 was observed even with NTP alone. At these lower input energies, the NO_x removal by the pathway represents in reactions (2, 3) may be more pronounced. Due to the partially high ozone production at these SIEs (Fig. 7), the existence of O radicals can generally be considered. Therefore, the lack of NO_x can be ruled out, since in the presence of O^* , there is a possibility of some reactions as the following³⁰⁻³²:

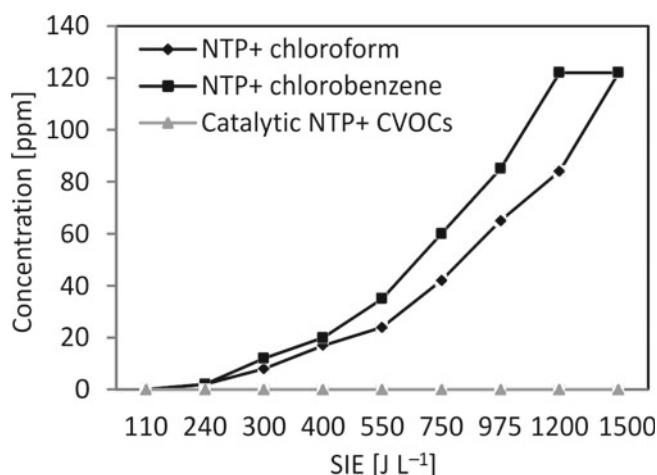


Figure 9. NO concentration detected downstream of NTP and catalyst reactor as a function of SIE

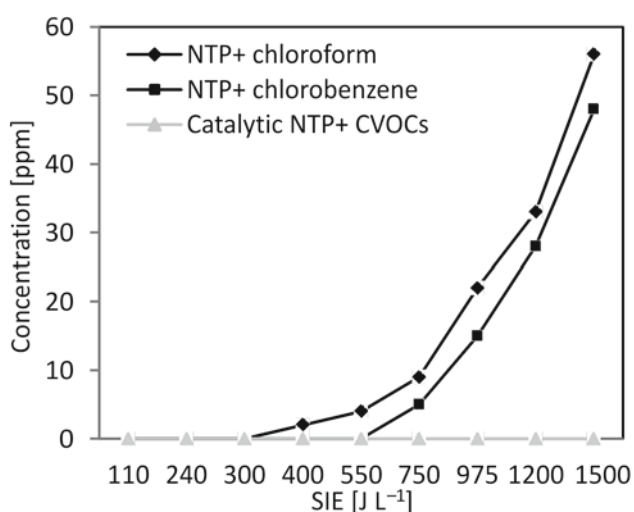
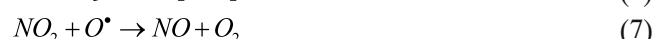
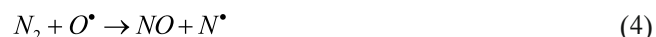


Figure 10. NO₂ concentration detected downstream of NTP and catalyst reactor as a function of SIE



Despite these points, Mok et al. recognized NO as an intermediate product that will be oxidized immediately through reaction (6) and some other routes, resulting in NO₂¹⁶.

Chlorinated by-products

The production of chlorinated by-products is inevitable during the decomposition of CVOCs inside a NTP reactor due to the generation of Cl[•] radicals. As a result, this issue has been highlighted by some researchers as a main drawback of destruction of CVOCs by NTP technology, since the decomposition of these compounds in an oxygen rich environment such as air can lead to the formation of products such as phosgene which are even more toxic than the original compounds^{33,34}. According to Indarto et al. and also Foglein et al., phosgene can be formed by the reaction between chlorine containing molecules and single O or radical O[•] as the following^{34,35}:



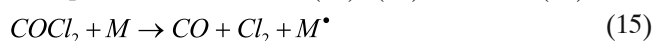
Phosgene is a high toxic compound and is not acceptable in the gas effluent due to environmental and occupational limit values. Catalyst incorporation can control the formation of phosgene and we noticed in the present study that when the catalyst was integrated, phosgene peaks were disappeared totally from mass spectrograms. The catalyst effect and the mechanism responsible for diminishing the selectivity level towards phosgene is not clearly known. It can be supposed that the presence of catalyst leads to a relatively higher quantities of reactive radicals such as O[•], OH[•], Cl[•], etc., which decompose COCl₂ totally and leave it as an intermediate product. Some of the decomposition pathways resulting from the reaction between COCl₂ and active radicals can be written as the following³³:



Due to the ozone destruction ability of the catalyst as mentioned above, the production of extremely higher level of O[•] radicals can be appreciated. As a result, the selectivity towards CO₂ and Cl₂ increases over the catalyst, according to the reaction (12). As far as the decomposition of chlorinated compounds containing more chlorine atoms such as chloroform is concerned, selectivity towards COCl₂ and Cl₂ is more pronounced^{33,36}:



In our experiments, with chloroform feeding both reactions (13) and (14) seem to play a significant role, since a high abundance was recorded for both compounds in mass spectrograms. In the presence of catalyst, however, reaction (14) appears to accelerate due to the higher concentration observed for Cl₂. Another reason may be resulted from the improved process of COCl₂ dissociation due to being attacked by more active radicals or excited molecules provided over the catalyst surface as expressed in reactions (10), (11) and also (15)³³:



According to previous works, besides phosgene, several other by-products can be generated^{35,37}. They are represented in Table 3, along with some of their properties. As can be seen from Table 3, HCl, CCl₄, Cl₂, dichloroacetylchloride (DCAC), trichloroacetaldehyde (TCAA), as well as COCl₂ were the predominant chlorinated by-products of NTP treatment. Some other compounds were also noticed by Futamura et al. and Evans et al.^{38,39} as represented in Table 3. Two products were observed during our tests that have not been reported by the previous works (trichlorobenzaldehyde (TCBA), and trichloroethylene (TCE)). The former is a heavy aldehyde compound, and although aldehydes are generally accepted to be water soluble, but the solubility of TCBA is not exactly known. The latter is a well-known air pollutant and has been the subject of decomposition by NTP itself in several cases^{40,41}. Contrary to the previous works, no CCl₄, DCAC, as well as methyl chloride were detected during the present study. Furthermore, the products detected by Futamura et al. were also not seen during our experiments. In addition, due to the difficulties of

Table 3. Major chlorinated by-products detected during this work and previous studies

By-product	Chemical formula	Water solubility	Molecular weight	Toxicity	m/z (GC/MS)	Reference
Hydrogen chloride	HCl	Very high	36.4	Corrosive	36	4; 16; 35; 46; This work
Carbon tetrachloride	CCl ₄	Low	153	Damaging to the liver	47-82-117	34; 35
Chlorine	Cl ₂	High	70.9	Irritant	35-70-74	4; 15; 16; 34-36; 46; This work
Dichloroacetylchloride (DCAC)	C ₂ H ₂ Cl ₂ O	Reacts with water	147.4	Corrosive	35-48-63-76-83-87-111	15
Trichloroacetaldehyde (TCAA)	CCl ₃ CHO	High	147.4	Toxic for CNS	35-47-82-11-118-148	15; This work
Phosgene	COCl ₂	Very low	98.9	Irritant	35-63-98	15; 16; 34; 36; 46; This work
Methyl chloride	CH ₃ Cl	Low	50.4	Damaging to liver, kidney, and CNS	15-35-47-50	4
Trichlorobenzaldehyde (TCBA)	C ₇ H ₃ Cl ₃ O	Unknown	209.4	Corrosive	74-77-84-97-109-144-179-207-224	This work
Trichloroethylene (TCE)	C ₂ HCl ₃	Low	131.3	Toxic for CNS, and kidney	35-47-60-95-99-130-134	This work
Formyle chloride	CHOCl	Insoluble	64.4	Damaging to eye, skin, CNS	-	39
Pentachloroethane	Cl ₅ C ₂ H	Low	202.2	Toxic for CNS, and skin	35-47-60-83-95-117-121-130-165-171	38
Dichloroacetonitrile	Cl ₂ C ₂ HN	Insoluble	109.9	Irritant	35-38-47-74-82-86	38
Tetrachloroethylene	Cl ₄ C ₂	High	165.8	Irritant	35-47-59-82-94-129-133-164-166-170	38
Chloroacetylene	ClC ₂ H	Low	60.4	Irritant	25-35-47-60	38

HCl detection by GC/MS in the presence of other chlorinated molecules resulting from the interferences with other compounds such as Cl₂, TCAA, TCE, and even COCl₂⁴⁰, we noticed no spectrogram for HCl during our tests. However, HCl can be produced through several reaction pathways resulting from direct decomposition of CVOCs as given by reactions (7), (9), and also from dissociation of intermediates^{4, 16}:



Production of HCl can particularly be appreciated with the hybrid system. As previously mentioned (reaction 11), HCl can be a probable consequence of destruction of COCl₂ which was totally removed with the hybrid TiO₂-ZnO/NTP during the present study. In this respect, effluent gas analysis employing several HCl detector tubes revealed a high concentration of hydrogen chloride. HCl generation may be even more concerned when a hydrogen-rich substance such as toluene is added to the reactor. Addition of methane-like compounds is recommended where CVOCs contain more chlorine than hydrogen atoms¹.

The initial gas feeding can dramatically influence the by-products distribution. In our study we noticed that with chloroform introduction a high concentration of COCl₂ appeared with NTP-alone process. Furthermore, the amount of Cl₂ was also considerable with chloroform feeding. These findings can be well supported by the observations of Marotta et al.²³. They reported that the negative species due to CHCl₃ dissociation are dominated by Cl⁻ ions either alone or in combination with background molecules such as H₂O. However, with chlorobenzene, the concentration of TCBA was more noticeable, followed by some amounts of Cl₂ and TCAA. Some heavy products were also appeared with chloroform in our study including TCAA, and TCE. Furthermore, some amounts of solid products were detected with both contaminants during the present study. This was observed

from an impinger trap located downstream of the set-up system and was supported by the study of Kovac et al.⁴² and Vandenbroucke et al.¹¹.

Due to the better effect of TiO₂-ZnO/GAC compared to TiO₂/GAC and ZnO/GAC, we investigated the influence of its hybrid with NTP to realize what happened with by-products distribution. Typical chlorinated by-products detected during our experiments with or without catalyst are shown in Table 4. In the present of TiO₂-ZnO/GAC, as we observed, COCl₂ was removed totally. Furthermore, in the case of chloroform, the concentration of TCBA and TCE decreased and the amount of TCAA, HCl, and Cl₂ soared up significantly instead. With chlorobenzene, however, TCBA (the main by-product) declined in favor of Cl₂, CO, and CO₂. A high concentration of HCl was also obtained with chlorobenzene feeding.

The chlorine balance value of 100% was not achievable even with the hybrid system. In the case of chloroform conversion at the highest applied SIE and downstream of the NTP-catalyst, the Cl₂ and HCl selectivity were calculated to be 47% and 24%, respectively. For chlorobenzene degradation and under the same conditions, however, the values were obtained 55% and 19% respectively. Other chlorinated by-products were not quantified, but due to a very low abundance of these undistinguished products on mass spectrograms, they are estimated to form only a few percent of end products.

Several works on CVOCs removal by NTP technology reported different selectivity towards chlorinated by-products^{21, 39, 43}. Oda et al. tried to decompose TCE and found DCAC and TCAA as main products with both NTP alone and hybrid process¹⁵. They reported that increasing the NTP power influenced TCAA formation positively and was associated with the decline of this chlorinated by-product. They also implied that the TCAA production may not be affected by the MnOx catalyst. However, we noticed that the hybrid process

Table 4. Chlorinated by-products detected during this work with and without catalyst

By-product	NTP-alone		Catalytic NTP	
	chloroform	chlorobenzene	chloroform	chlorobenzene
Hydrogen chloride	✓	✓	✓	✓
Chlorine	✓	✓	✓	✓
Trichloroacetaldehyde	✓	–	✓	✓
Phosgene	✓	✓	–	–
Trichlorobenzaldehyde	✓	✓	✓	✓
Trichloroethylene	✓	–	–	–

affected efficiently the production of TCAA, and raising the plasma power (NTP-alone) yielded more TCAA and other by-products formation due to further dissociation of initial CVOCs. Magureanu et al investigated the conversion of TCE in a DBD reactor and found some heavy hydrocarbons including decanal and nonanal as probable end products²¹, while such compounds were noticed neither by other studies nor by the present work. However, they reported Cl₂ and HCl as predominant final products which can be in good agreement with the current work. These authors also discussed the effect of MnO_x on by-products formation and found it to have a beneficial effect on total removal of compounds like DCAC and TCAC. No work was found in the literature on the hybrid catalytic plasma for chloroform and chlorobenzene conversion. However, the removal of these compounds has been investigated by the NTP-alone process in few studies^{16, 23, 44, 45}. Mok et al. decomposed chloroform using two kinds of NTP reactors i.e. DBD and packed bed and noted the existence of some species such as Cl₂O, HOCl, NCl, etc. as part of the final products in the effluent gas¹⁶. The production of these compounds has never been mentioned in previous works. Despite this, the authors reported Cl₂, HCl, and COCl₂ as main by-products and no heavy molecule was detected by them as end product. But, due to the low chlorine balance that they informed in their study, the presence of some heavy molecules could be also considered. No chlorinated by-product was reported by Sivachandiran et al. in their study on chlorobenzene destruction performed applying two configurations of DBD⁴⁴, and also by Snyder et al using a coaxial DBD reactor⁴⁵.

In accordance with the all above-mentioned, one can conclude that even with the hybrid catalytic NTP, the production of some unwanted chlorinated by-products is inevitable. Among these by-products, Cl₂ and HCl are desirable and less harmful^{1, 39}. They are water-soluble and can be removed totally using a wet scrubber downstream of the convertor system. Since the solubility of TCAA is high, it may also be a favorable product, while TCBA may not be a desirable one. Addition of hydrogen containing compounds may be suggested to shift the reactions towards HCl and Cl₂. Combining a suitable catalyst for further decomposition of TCBA and some other heavy products may also be the subject of future works.

CONCLUSION

TiO₂, ZnO, and mixture of TiO₂-ZnO impregnated on GAC prepared by sol-gel technique were coupled with NTP in order to investigate their catalytic activity on the by-product distribution of chloroform and chlorobenzene. The formation of harmful chlorinated by-products was decreased significantly with the hybrid technique. NO, NO₂, O₃, and COCl₂ were removed totally, and CO₂

and H₂O soared up considerably instead. The amount of some hazardous compounds such as CO, and trichloroacetaldehyde was still high even with catalyst integration. However, trichlorobenzaldehyde and trichloroethylene were further decomposed significantly with the hybrid process. The initial gas composition has a noteworthy influence on the by-products distribution and higher amounts of CO_x were obtained with chlorobenzene feeding.

ACKNOWLEDGMENT

The financial support for this work, which was part of Ph.D. thesis, comes from Hamedan University of Medical Sciences as Grant no. 9107252600.

LITERATURE CITED

- Ojala, S., Pitkäaho, S., Laitinen, T., Niskala Koivikko, N., Brahmī, R., Gaálová, J., Matejova, L., Kucherov, A., Päivärinta, S. & Hirschmann, C. (2011). Catalysis in VOC Abatement. *Top Catal.* 54, 1224–1256. DOI: 10.1007/s11244-011-9747-1.
- Humans, I. International agency for research on cancer. (1979). IARC monographs on the evaluation of the carcinogenic risk of chemicals to humans. From <http://monographs.iarc.fr/>
- Pitkäaho, S., Ojala, S., Kinnunen, T., Silvonen, R. & Keski, R.L. (2011). Catalytic Oxidation of Dichloromethane and Perchloroethylene: Laboratory and Industrial Scale Studies. *Top Catal.* 54, 1257–1265. DOI: 10.1007/s11244-011-9748-0.
- Iijima, S., Nakamura, M., Yokoi, A., Kubota, M., Huang, L. & Matsuda, H. (2011). Decomposition of dichloromethane and in situ alkali absorption of resulting halogenated products by a packed-bed non-thermal plasma reactor. *J. Mater. Cy Waste Manag.* 13, 206–212. DOI: 10.1007/s10163-011-0022-0.
- Pahwa, M., Demers, P. & Ge, C. (2012). Occupational exposure limits for carcinogens in Ontario workplaces: Opportunities to prevent and control exposure. From <http://occupationalcancer.ca/2012/occupational-exposure-limits-for-carcinogens-in-ontario-workplaces-opportunities-to-prevent-and-control-exposure/>
- Subrahmanyam, C., Renken, A. & Kiwi-Minsker, L. (2007). Novel catalytic non-thermal plasma reactor for the abatement of VOCs. *Chem. Eng. J.* 134, 78–83. DOI: 10.1016/j.cej.2007.03.063.
- Agnihotri, S., Cal, M.P. & Prien, J. (2004). Destruction of 1, 1, 1-trichloroethane using dielectric barrier discharge non-thermal plasma. *J. Environ. Eng.* 130, 349–355. DOI: 10.1061/(ASCE)0733-9372.
- Subrahmanyam, C., Magureanu, M., Laub, D., Renken, A. & Kiwi-Minsker, L. (2007). Nonthermal plasma abatement of trichloroethylene enhanced by photocatalysis. *J. Phys. Chem. C.* 111, 4315–4318. DOI: 10.1021/jp066731o.
- Subrahmanyam, C., Magureanu, M., Renken, A. & Kiwi-Minsker, L. (2006). Catalytic abatement of volatile organic compounds assisted by non-thermal plasma: Part 1. A novel dielectric barrier discharge reactor containing catalytic electrode. *Appl. Catal. B.* 65, 150–156. DOI: 10.1016/j.apcatb.2006.01.006.
- Mo, J., Zhang, Y., Xu, Q., Lamson, J.J. & Zhao, R. (2009). Photocatalytic purification of volatile organic compounds in indoor air: A literature review. *Atmos Environ.* 43, 2229–2246. DOI: 10.1016/j.atmosenv.2009.01.034.

11. Vandenbroucke, A.M., Dinh, M.T.N., Giraudon, J.M., Morent, R., De Geyter, N., Lamonier, J.F. & Leys, C. (2011). Qualitative by-product identification of plasma-assisted TCE abatement by mass spectrometry and Fourier-transform infrared spectroscopy. *Plasma Chem Plasma Proces.* 31, 707–718. DOI: 10.1007/s11090-011-9310-7.
12. Van Durme, J., Dewulf, J., Leys, C. & Van Langenhove, H. (2008). Combining non-thermal plasma with heterogeneous catalysis in waste gas treatment: A review. *Appl. Catal. B.* 78, 324–333. DOI: 10.1016/j.apcatb.2007.09.035.
13. Chen, H.L., Lee, H.M., Chen, S.H., Chang, M.B., Yu, S.J. & Li, S.N. (2009). Removal of volatile organic compounds by single-stage and two-stage plasma catalysis systems: a review of the performance enhancement mechanisms, current status, and suitable applications. *Environ. Sci. Technol.* 43, 2216–2227. DOI: 10.1021/es802679b.
14. Augugliaro, V., Loddo, V., Palmisano, G., Palmisano, L. & Pagliaro, M. (2010). *Clean by light irradiation*. RSC Pub. Royal Society of Chemistry.
15. Oda, T., Kuramochi, H. & Ono, R. (2008). Trichloroethylene decomposition by the nonthermal plasma Combined with manganese-dioxide supported alumina. *Int. J. Plasma Environ. Sci. Technol.* 2, 50–55. DOI: 10.1541/ieejfms.127.145.
16. Mok, Y., Lee, S.B., Oh, J.H., Ra, K.S. & Sung, B.H. (2008). Abatement of trichloromethane by using nonthermal plasma reactors. *Plasma Chem Plasma Proces.* 28, 663–676. DOI: 10.1007/s11090-008-9151-1.
17. Indarto, A., Choi, J.-W., Lee, H. & Song, H.K. (2006). Treatment of CCl₄ and CHCl₃ emission in a gliding-arc plasma. *Plasma Devices Oper.* 14, 1–14. DOI: 10.1080/10519990500493833.
18. Hu, Y. & Yuan, C. (2006). Low-temperature preparation of photocatalytic TiO₂ thin films on polymer substrates by direct deposition from anatase sol. *J. Mater. Sci. Technol.* 22, 239–244. DOI: 10.1016/j.jcrysgro.2004.10.146.
19. Carp, O., Huisman, C. & Reller, A. (2004). Photoinduced reactivity of titanium dioxide. *Progr. Sol. Stat. Chem.* 32, 33–177. DOI: 10.1016/j.progsolidstchem.2004.08.001.
20. Liu, Y., Yang, S., Hong, J. & Sun, C. (2007). Low-temperature preparation and microwave photocatalytic activity study of TiO₂-mounted activated carbon. *J. Haz. Mat.* 142, 208–215. DOI: 10.1016/j.jhazmat.2006.08.020.
21. Magureanu, M., Mandache, N., Parvulescu, V., Subrahmanyam, C., Renken, A. & Kiwi-Minsker, L. (2007). Improved performance of non-thermal plasma reactor during decomposition of trichloroethylene: Optimization of the reactor geometry and introduction of catalytic electrode. *Appl. Catal. B.* 74, 270–277. DOI: 10.1016/j.apcatb.2007.02.019.
22. Twigg, M.V. (2006). Roles of catalytic oxidation in control of vehicle exhaust emissions. *Catal Today.* 117, 407–418. DOI: 10.1016/j.cattod.2006.06.044.
23. Marotta, E., Scorrano, G. & Paradisi, C. (2005). Ionic reactions of chlorinated volatile organic compounds in air plasma at atmospheric pressure. *Plasma Process Polym.* 2, 209–217. DOI: 10.1002/ppap.200400047.
24. Francke, K.P., Miessner, H. & Rudolph, R. (2000). Cleaning of air streams from organic pollutants by plasma-catalytic oxidation. *Plasma Chem Plasma Proces.* 20, 393–403. DOI: 10.1023/A:1007048428975.
25. Kim, H.H. & Ogata, A. (2011). Nonthermal plasma activates catalyst: from current understanding and future prospects. *European Phys. J. App. Phys.* 55. DOI: 10.1051/epjap/2011100444.
26. Karuppiah, J., Reddy, E.L., Reddy, P.M.K., Ramaraju, B. & Subrahmanyam, C. (2013). Catalytic nonthermal plasma reactor for the abatement of low concentrations of benzene. *Int. J. Environ. Sci. Technol.* 1–8. DOI: 10.1007/s13762-013-0218-z.
27. Matsumoto, S.J. (2000). Catalytic reduction of nitrogen oxides in automotive exhaust containing excess oxygen by NOx storage-reduction catalyst. *Cattech* 4, 102–109. DOI: 10.1023/A:1011951415060.
28. Kang, C.S., You, Y.J., Kim, K.J., Kim, T.h., Ahn, S.J., Chung, K.H., Park, N.C., Kimura, S. & Ahn, H.G. (2006). Selective catalytic reduction of NOx with propene over double wash-coat monolith catalysts. *Catal Today.* 111, 229–235. DOI: 10.1016/j.cattod.2005.10.031.
29. Shelef, M. (1995). Selective catalytic reduction of NOx with N-free reductants. *Chem. Review.* 95, 209–225. DOI: 10.1021/cr00033a008.
30. Centi, G., Ciambelli, P., Perathoner, S. & Russo, P. (2002). Environmental catalysis: trends and outlook. *Catal Today.* 75, 3–15. DOI: 10.1016/S0920-5861(02)00037-8.
31. Roy, S., Hegde, M. & Madras, G. (2009). Catalysis for NOx abatement. *Applied Energy.* 86, 2283–2297. DOI: 10.1016/j.apenergy.2009.03.022.
32. Ozawa, Y. & Urashima, K. (2006). *Recent Development Trends in Catalyst Technologies for Reducing Nitrogen Oxide Emissions*. Science and Technology Trends.
33. Lee, W.J., Chen, C.Y., Lin, W.C., Wang, Y.T. & Chin, C.J. (1996). Phosgene formation from the decomposition of 1, 1-C₂H₂Cl₂ contained gas in an RF plasma reactor. *J. Haz. Mat.* 48, 51–67. DOI: 10.1016/0304-3894(95)00145-X.
34. Indarto, A., Choi, J.-W., Lee, H. & Song, H.-K. (2006). Decomposition of CCl₄ and CHCl₃ on gliding arc plasma. *J. Environ. Sci.* 18, 83–89. DOI: 1001-0742(2006)01-0083-07.
35. Föglein, K.A., Szabó, P.T., Babievskaya, I.Z. & Szépvölgyi, J. (2005). Comparative study on the decomposition of chloroform in thermal and cold plasma. *Plasma Chem Plasma Proces.* 25, 289–302. DOI: 10.1007/s11090-004-3041-y.
36. Indarto, A., Choi, J.W., Lee, H. & Song, H.K. (2008). Decomposition of greenhouse gases by plasma. *Environ. Chem. Letters.* 6, 215–222. DOI: 10.1007/s10311-008-0160-3.
37. Schmidt-Szałowski, K., Krawczyk, K., Sentek, J., Ulejczyk, B., Górka, A. & Młotek, M. (2011). Hybrid plasma-catalytic systems for converting substances of high stability, greenhouse gases and VOC. *Chem. Eng. Res. Design.* 89, 2643–2651. DOI: 10.1016/j.cherd.2011.06.018.
38. Futamura, S. & Yamamoto, T. (1997). Byproduct identification and mechanism determination in plasma chemical decomposition of trichloroethylene. *IEEE T Industry Applications.* 33, 447–453. DOI: 10.1109/28.568009.
39. Evans, D., Rosocha, L.A., Anderson, G.K., Coogan, J.J. & Kushner, M.J. (1993). Plasma remediation of trichloroethylene in silent discharge plasmas. *J. Appl. Phys.* 74, 5378–5386. DOI: 10.1063/1.354241.
40. Vandenbroucke, A., Morent, R., De Geyter, N. & Leys, C. (2011). Decomposition of Trichloroethylene with Plasma-catalysis: A review. *J. Adv. Oxid. Technol.* 14, 165–173.
41. Nakagawa, Y., Fujisawa, H., Ono, R. & Oda, T. (2010). Dilute Trichloroethylene Decomposition by using High Pressure Non-Thermal Plasma: Humidity Effects. In *Industry Applications Society Annual Meeting (IAS)*, IEEE. pp 1–4.
42. Kovács, T., Turányi, T. & Szépvölgyi, J. (2010). CCl₄ Decomposition in RF Thermal Plasma in Inert and Oxidative Environments. *Plasma Chem Plasma Proces.* 30, 281–286. DOI: 10.1007/s11090-010-9219-6.
43. Han, S.-B. & Oda, T. (2007). Decomposition mechanism of trichloroethylene based on by-product distribution in the hybrid barrier discharge plasma process. *Plasma Sour. Sci. Technol.* 16, 413. DOI: 10.1088/0963-0252/16/2/026.
44. Sivachandiran, L., Karuppiah, J. & Subrahmanyam, C. (2012). DBD plasma reactor for oxidative decomposition of Chlorobenzene. *Int. J. Chem. React. Eng.* 10. DOI: 10.1515/1542-6580.2785.
45. Snyder, H.R. & Anderson, G.K. (1998). Effect of air and oxygen content on the dielectric barrier discharge decomposition of chlorobenzene. *IEEE T Plasma Sci.* 26, 1695–1699. DOI: 10.1109/27.747888.
46. Magureanu, M., Mandache, N. & Parvulescu, V. (2007). Chlorinated organic compounds decomposition in a dielectric barrier discharge. *Plasma Chem Plasma Process.* 27, 679–690. DOI: 10.1007/s11090-007-9103-1.